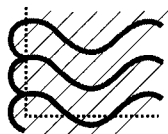


Chapter 5



Polymer Gels

5.1 INTRODUCTION

Gelation is the conversion of a liquid to a disordered solid by formation of a network of chemical or physical bonds between the molecules or particles composing the liquid. The liquid precursor is called the “sol,” and the solid formed from it is the “gel.” Gels can be as mundane as the epoxy glue used to mend a child’s toy, or they can be as sublime as the jellies, meringues, and custards that delight the mavens of haute cuisine.

This chapter is devoted to the properties of *polymeric* gel-forming liquids. Particulate gels are discussed in Chapter 7. The structure of a polymeric gel is sketched in Fig. 5-1. Since this book is devoted to materials that are in some sense liquid, or at least liquefiable, we shall not say much about hard, irreversible, chemical gels such as cured epoxies or vulcanized rubber, but shall focus instead on chemical *pre-gels* and thermally reversible *physical gels*, both of which can be considered borderline fluids. This chapter is confined to a brief overview. Much more detail can be found in Winter and Mours (1997), and volume 101 of the *Faraday Discussions*.

Crucial to the formation of such gels is *branching* or *multifunctionality*. The functionality f of a molecule is the number of bonds it can form with other molecules; $f = 4$ in Fig. 5-1.

There are at least three generic types of *chemical* reaction that can produce such branching structures (de Gennes 1979). The first is a *condensation reaction*, whereby a molecule with three or more reactive groups, such as OH groups, reacts with a *cross-linker*. A second type of branching reaction is *addition* polymerization, whereby a double bond is opened by a free-radical reaction, creating additional bonds that link monomers together. This type of reaction will produce linear chains if there is only one double bond per monomer, but if there are two or more double bonds, branching can occur. The third way to create branching is to start with linear polymeric precursors, and *cross-link* or *vulcanize* them by introducing chemical links that bond them together. For an explanation of the chemistry of gelation, see Flory (1953).

Physical gelation occurs as a result of *intermolecular association*, leading to network formation (see Fig. 5-2). (Physical associations differ from chemical bonds in that the latter are covalent attachments between two atoms and are typically permanent at temperatures of interest here, while intermolecular associations are weak, reversible bonds or clusters produced by van der Waals forces, electrostatic attractions, or hydrogen bonding.) If physical associations are to produce gelation, rather than phase separation, it is crucial

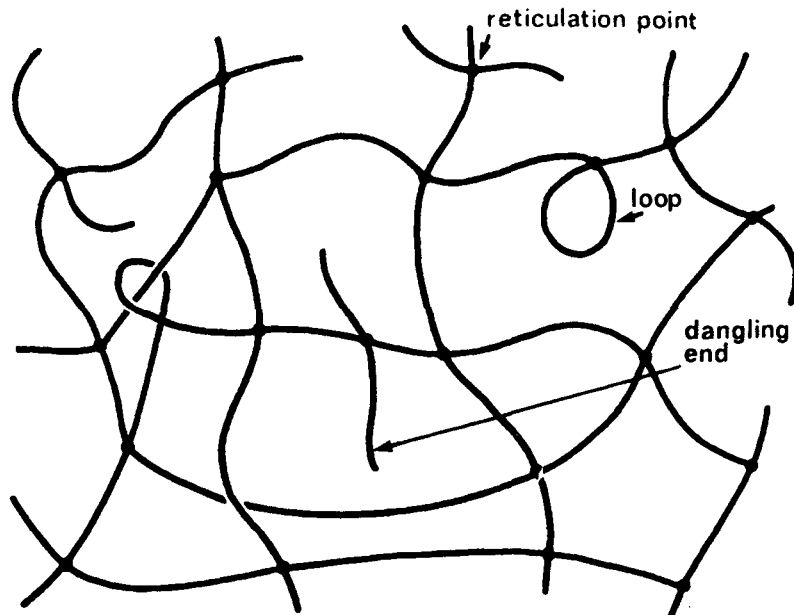


Figure 5.1 A typical polymer gel network. (Reprinted from Pierre-Gilles de Gennes, *Scaling Concepts in Polymer Physics*. Copyright © 1979 by Cornell University. Used by permission of the publisher, Cornell University Press.)

that the junctions between molecules that are formed by such associations do not grow too large. Thus, there must be some means of frustrating the growth of these associating domains, so that their size is limited. de Gennes identifies three types of interactions that can lead to physical gelation: (1) local *helical structures* whereby one molecule winds around another; (2) *microcrystallites*; and (3) *nodular domains*, in which the chain is chemically heterogeneous, and association only occurs at preferred sites along the chain. Examples of polymers that form nodular domains include water-soluble *associative thickeners*, which contain *hydrophobic* sites along an otherwise hydrophilic chain. At low concentrations, such thickeners greatly enhance the viscosity of water, and thus they are useful as additives to foods, shampoos, and other personal care products (see Fig. 1-4), or as mobility control agents in oil-field production. They form “flowable networks” that can, for example, be deposited in a capillary tube and used for electrophoretic separation of DNA (Menchen and Winnik 1994; Menchen et al. 1996). The reverse kind of associating polymer also exists—that is, hydrophobic molecules with hydrophilic sites, such as hydrogen-bonding or ionic groups. Peculiar rheological phenomena, such as “shear-induced gelation,” have been ascribed to intermolecular “associations” for many years (Eliassaf et al. 1955; Lodge 1961; Peterlin and Turner 1965), but only recently has any detailed microscopic understanding been achieved. Further discussion of physical gelation is deferred to Section 5.4. More detail can be found in the book by Guenet (1992).

Because gels are disordered materials that are kinetically frozen, the method of preparation strongly influences the properties obtained. For example, a gel prepared in a “dry”

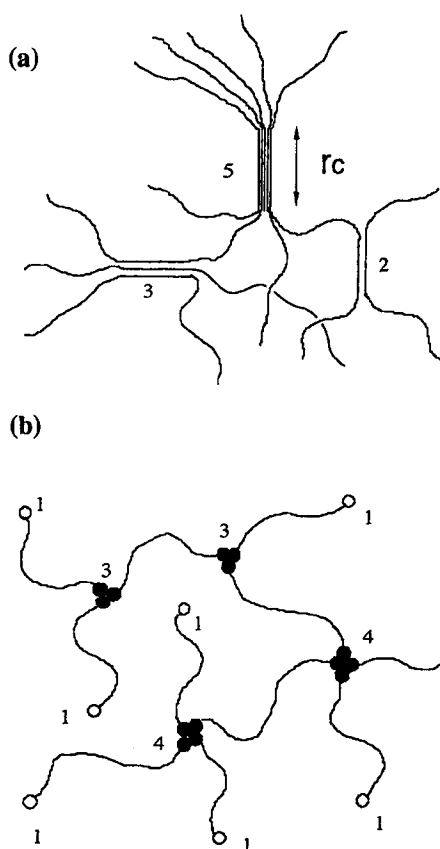


Figure 5.2 Illustrations of physical gels. In (a), the junctions are formed by microcrystallites, while in (b) the junctions are formed by the end groups of telechelic polymers. The functionalities of the various cross-link points are indicated by numbers beside the junctions. (Reprinted with permission from Tanaka and Stockmayer, *Macromolecules* 27:3943. Copyright 1994 American Chemical Society.)

state, with no solvent present, and then swollen by introduction of a solvent, will have a modulus that differs from that of a gel cross-linked with the solvent already present. Similar sensitivity to preparation conditions is found in physical gels. As a result, experiments on gels tend to be difficult to reproduce with precision.

Gels are indeed often prepared in the presence of a solvent, which is then removed to produce a solid with commercially valuable properties. If the solvent is removed by evaporation under normal conditions, the gel structure usually shrinks because of capillary forces acting on the liquid–air menisci. This produces a dense material with moderate or low porosity called a *xerogel*. On the other hand, if the solvent is removed by supercritical drying which prevents liquid–air menisci from forming, the product is an *aerogel*, which can have a solids volume fraction as low as 1% (Brinker and Scherer 1990).

Some polymeric gels with charged groups along their backbones can, when immersed in hydrophilic media, shrink or expand enormously in response to a change in temperature, pH, or electric field (Tanaka 1981; Osada and Ross-Murphy 1993). It has been proposed that such “intelligent gels,” if they could be made to respond quickly enough to an electric field or temperature, might serve as “artificial muscles” (Osada and Ross-Murphy 1993; Hu et al. 1995b).

5.2 GELATION THEORIES

5.2.1 Percolation Theory

Stauffer (1976) and de Gennes (1976, 1979) have pointed out the connection between gelation and *bond percolation*. To illustrate, let each site (or lattice points) on the square lattice in Fig. 5-3 represent a polyfunctional molecular unit, and let each filled link represent a chemical bond between neighboring units. Chemical reaction then corresponds to the conversion of unfilled bonds to filled bonds. As one increases the fraction p of bonds that are filled, more and more units link together, producing *clusters* of bonds; and eventually, at the *percolation transition*, $p = p_c$ (which corresponds to the gel point), an infinite, lattice-spanning cluster appears. Generally speaking, *percolation* is the process of network formation by random filling of bonds (or sites) on a lattice, or by random

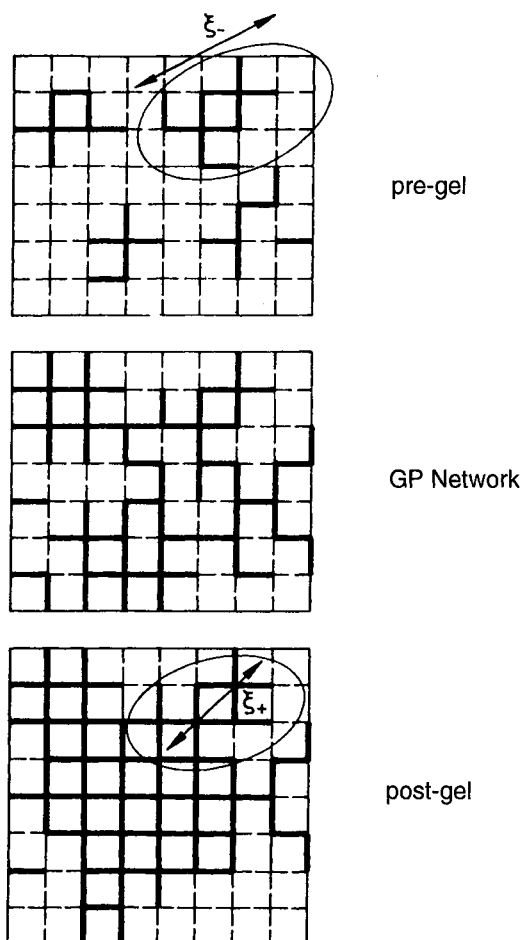


Figure 5.3 Typical configuration of closed bonds resulting from random filling of a square lattice. At small fractions p of filled bonds there are only isolated clusters whose correlation length is ξ_- ; when p exceeds the percolation threshold p_c , a sample-spanning cluster appears. The correlation length ξ is infinite at p_c and is finite both above and below it. (From Hess et al. 1988), (reprinted with permission from Hess et al., *Macromolecules* 21:2536. Copyright 1988 American Chemical Society.)

filling of regions of space (Broadbent and Hammersley 1957; Kirkpatrick 1973). For bond percolation on a square, $p_c = 0.5$. On other 2-D lattices, one finds empirically that $p_c \approx 2/z$, where z is the lattice coordination number; on 3-D lattices, $p_c \approx 1.5/z$ (Shante and Kirkpatrick 1971; Brinker and Scherer 1990). Although in a gelling system there are molecular diffusive motions and other complications, percolation theory nevertheless provides useful predictions, especially for properties near the gel point.

5.2.2 Flory–Stockmayer Theory

An earlier way of viewing gelation is due to Flory (1941, 1942) and Stockmayer (1943). In this *classical* theory, one also considers the buildup of large clusters by random bonding, but loops or cycles are ignored. Thus, the bonding process is effectively *tree-like*, as depicted in Fig. 5-4. Each new branch of the tree has as much freedom to grow new branches as its predecessor, without restrictions due to excluded volume or cycle formation. Because of the absence of closed cycles, the statistical properties of tree-like clusters can be computed analytically (Fisher and Essam 1961; Stinchcombe 1974; Larson and Davis 1982; Straley 1977, 1982), which makes the Flory–Stockmayer model a very convenient one that captures the essence of the gelation process.

The gel point in the classical theory is

$$p_c = \frac{1}{f - 1}$$

where f is the coordination number of the tree—that is, the number of bonds that can form at each site of the network (Flory 1953). If the gel is formed by reacting precursor molecules (A) with a chemical cross-linkers (B), then the gel point, measured as a fraction $p_{c,A}$ of A's reaction sites, depends on the functionalities (f_A and f_B) of both A and B as

$$p_{c,A} = \frac{1}{\sqrt{(f_A - 1)(f_B - 1)/r}}$$

where r is the “stoichiometric ratio” of B to A reactive sites:

$$r \equiv \frac{f_B n_B}{f_A n_A}$$

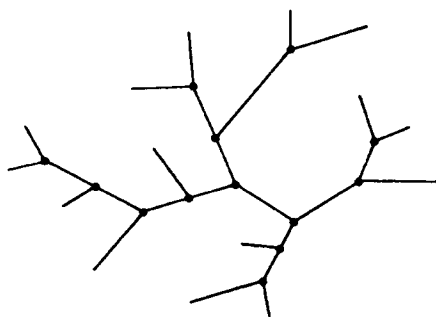


Figure 5.4 Illustration of a tree-like gel cluster. (Reprinted from Pierre-Gilles de Gennes, *Scaling Concepts in Polymer Physics*. Copyright © 1979 by Cornell University. Used by permission of the publisher, Cornell University Press.)

where n_A and n_B are the number of moles of A and B in the reactive mixture. Despite the limitations of the classical theory (e.g., the neglect of loops), the above formula for p_c seems to be reasonably accurate (Vallés and Macosko 1979; Venkataraman et al. 1989).

In the classical theory, however, the neglect of loops significantly affects the size distribution and other properties of the clusters as one approaches the gel point. Some of the “critical exponents” that describe these properties in the classical theory and in percolation theory near $p = p_c$ are compiled in Table 5-1 (Martin and Adolf 1991).

In Table 5-1, $\varepsilon \equiv |p - p_c|$, $N(m)$ is the number of clusters containing m bonds, R is the radius of a cluster of molecular weight M , and M_z and M_w are the z -averaged and weight-averaged molecular weights of the clusters, namely,

$$M_z = \frac{\sum m^3 N(m)}{\sum m^2 N(m)}, \quad M_w = \frac{\sum m^2 N(m)}{\sum m N(m)} \quad (5-1)$$

When $p > p_c$, one can define $P(p)$ to be the fraction of bonds belonging to the infinite cluster. The percolation predictions of the modulus G , the longest relaxation time τ , and the viscosity η depend on whether one uses the Rouse–Zimm (R–Z) theory, or the analogy to an electrical network (EN). The exponent for the modulus G is predicted to be greater than either of these (i.e., around 3.7) if bond-bending dominates (Arbabi and Sahimi 1988). Further details about these exponents can be found in Chapter 5 of Brinker and Scherer (1990), as well as in Martin and Adolf (1991).

5.2.3 Fractals and Self-Similarity

The power-law scaling of the cluster properties shown in Table 5-1 arises from their *fractal* or *self-similar* character. Self-similarity implies that the huge clusters formed near the gel point look the same at any magnification, as long as elementary units making up the cluster are too small to see. Furthermore, the cluster size distribution at one value of $\varepsilon(\varepsilon_1)$ is the

TABLE 5-1
Scaling Exponents for Classical and Percolation Theories of Gelation

Exponent	Relation	Classical	3-D Percolation		Experimental
λ	$N(m) \sim m^{-\lambda}$	5/2	2.20		2.18–2.3
σ	$M_z \sim \varepsilon^{-1/\sigma}$	1/2	0.45		—
γ	$M_w \sim \varepsilon^{-\gamma}$	1	1.76		1.0–2.7
ν	$R_z \sim \varepsilon^{-\nu}$	1	0.89		—
D_f	$R^{D_f} \sim M$	4	2.5		1.98
β	$P \sim \varepsilon^\beta$	1	0.39		—
			R–Z	EN	
t	$G \sim \varepsilon^t$	3	2.7	1.94	1.9–3.5
ζ	$\tau \sim \varepsilon^{-\zeta}$	3	4.0–2.7	2.6	3.9
$k = \zeta - t$	$\eta \sim \varepsilon^{-k}$	0	0–1.35	0.75	0.75–1.5

same as at a smaller value of $\varepsilon(\varepsilon_2)$, if one uniformly magnifies in size all clusters formed at ε_1 . The exponent D_f in Table 5-1 is called the *fractal dimension* of the cluster; it is the exponent relating the linear size to the mass. For any dense three-dimensional ($D = 3$) object, this exponent is $D_f = D = 3$; clusters with $D_f < D$ are ramified, open structures.

5.3 RHEOLOGY OF CHEMICAL GELS AND NEAR-GELS

When a precursor liquid, composed of either small molecules or polymers, is cross-linked to form a gel, the rheological properties change from those of a viscous liquid to those of an elastic solid. Thus, at the gel point, the viscosity of the liquid diverges to infinity, and the low-frequency modulus G_0 rises from zero, as shown schematically in Fig. 5-5. The modulus of the fully cured elastic solid can be estimated as (Wall 1943; Treloar 1975)

$$G_0 = \nu kT \quad (5-2)$$

where ν is the number of “elastically effective” network strands per unit volume. Equation (5-2) assumes that the cross-link points or junctions of the network move *affinely*, or in proportion to, the macroscopic strain. This is only expected to occur when the functionality of the network is high. For low functionality, the junctions are liable to move nonaffinely to produce a lower overall stress. If the junctions and the chains can move nonaffinely without interfering with each other (i.e., they are so-called phantom chains), then ν in Eq. (5-2) should be replaced by $\nu - \mu$, where μ is the number of junctions per unit volume (James and Guth 1953; Ferry 1980). Erman and Flory (1983) have developed equations for the more realistic case of “constrained junction fluctuations.” Additional prefactors

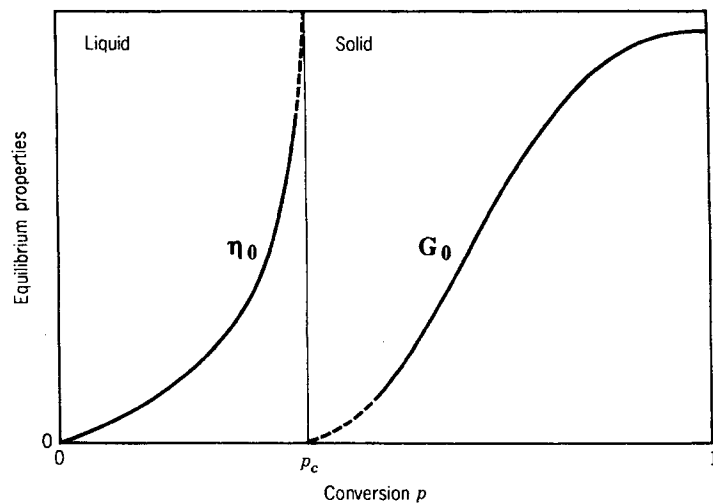


Figure 5.5 Illustration of the dependence of zero-shear viscosity η_0 and equilibrium modulus G_0 on conversion p for a cross-linking system. (From Winter, *Encyclopedia of Polymer Science and Engineering*, Copyright © 1989. Reprinted by permission of John Wiley & Sons, Inc.)

can be introduced into Eq. (5-2) due to the presence of “trapped entanglements” and other considerations (Ferry 1980). In addition, “dangling ends” that are not “elastically effective” must be excluded from ν . Near the gel point, such “ineffective” bonds are common, and the gel modulus typically follows a power law $G \sim |p - p_c|^f$ as indicated in Table 5-1.

At large deformations, outside the linear regime, the stress tensor for a polymer gel, according to the classical affine-motion rubber-elasticity theory (Section 3.4.2), is

$$\boldsymbol{\sigma} = G_0 \mathbf{B} \quad (5-3)$$

where \mathbf{B} is the *Finger tensor* defined in Eq. (1-16).

Equation (5-3) does not describe real gels very well. The empirical *Mooney–Rivlin* expression (Mooney 1940; Rivlin 1948; Treloar 1975) does better:

$$\boldsymbol{\sigma} = 2C_1 \mathbf{B} + 2C_2 \mathbf{C} \quad (5-4)$$

where $\mathbf{C} \equiv \mathbf{B}^{-1}$ is the Cauchy tensor, the inverse of the Finger tensor, and C_1 and C_2 are empirical constants tabulated for various polymer gels by Horkay and McKenna (1996).

Further discussion of models of the elasticity of gels is beyond the scope of the present work; the interested reader can find a thorough description of the elasticity and viscoelasticity of polymer chemical gels in Ferry (1980), Treloar (1975), and Flory (1953).

More relevant to this book on complex *fluids* are the properties of the partially gelled liquids formed on the way toward complete gelation. The rheology of partially cured materials has been studied in detail by Winter, Chambon, and coworkers (Chambon et al. 1986; Winter and Chambon 1986; Winter et al. 1988; Scanlan and Winter 1991; Izuka et al. 1992; Richtering et al. 1992). Such partially cured or lightly cross-linked materials not only are scientifically interesting, but also are technologically important, for example as *adhesives*. Their rheology is intermediate between fluid and solid, making them sticky or *tacky* (Winter 1989; Zosel 1991).

Figure 5-6 shows the storage and loss modulus, at a fixed frequency, for poly(dimethylsiloxane) cross-linked with a tetrasilane cross-linker, as a function of reaction time. At short times after the start of cross-linking, the material is a liquid with $G'' \gg G'$; but as the reaction continues, the storage modulus rises from close to zero toward a long-time asymptote of around 10^5 Pa. At the point marked t_c , the storage and loss moduli cross each other, marking a transition from liquid-like to solid-like behavior. These measurements were made after quenching the reaction at various times after the start of the reaction. Quenching can be avoided for photocurable samples cured in the rheometer with transparent fixtures [see Chiou et al. (1996)].

Figure 5-7 shows the frequency dependences of the storage and loss moduli at various times during the reaction, from 6 minutes before t_c to 6 minutes after it. Note that at t_c (labeled “Gel Point” in Fig. 5-7), G' and G'' follow *power laws* over the entire frequency range! For times less than this (labeled -2 and -6 in Fig. 5-7), the curves slope downward at low frequencies, which is indicative of fluid-like behavior, while at times after the “gel point” (labeled $+2$ and $+6$), G' flattens at low frequency—a characteristic of solid-like behavior. Thus, the intermediate state with a power-law frequency dependence over the whole frequency range is the transitional state between liquid-like and solid-like behavior, and therefore it defines the gel point. This rheologically determined gel point coincides with the conventional value, namely the maximum degree of cure at which

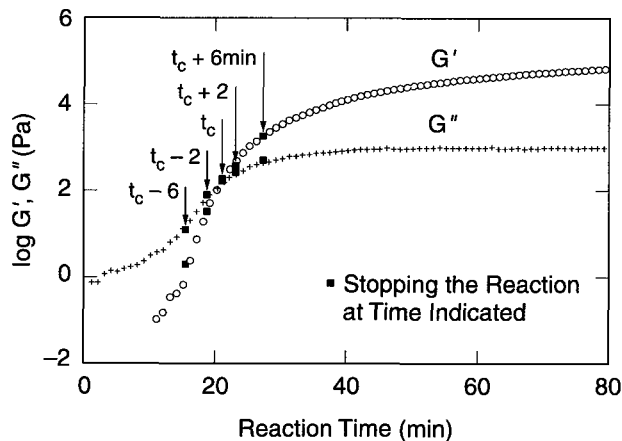


Figure 5.6 Time-dependence of G' (\circ) and G'' ($+$) during cross-linking reaction of sub-entangled poly(dimethylsiloxane) at balanced stoichiometry with a tetrasilane crosslinker. The gel point is marked as t_c . (From Winter and Chambon 1986, with permission from the Journal of Rheology.)

the partially cross-linked system still dissolves completely in a good solvent (Winter et al. 1988).

The relaxation modulus of the transitional state at the gel point is therefore described by a simple power law:

$$G(t) = St^{-n} \quad (5-5)$$

where S is called the *strength* of the gel. The exponent n in Eq. (5-5) is 0.5 for the data in Figs. 5-6 and 5-7. It has been found to vary over the wide range 0.19–0.92 for chemically cross-linking systems (Scanlan and Winter 1991), with even lower values of n in some physically gelling systems (Richtering et al. 1992). By the Kramers–Kroenig relationship, Eq. (5-5) implies that

$$G'(\omega) = \frac{G''(\omega)}{\tan(n\pi/2)} = \Gamma(1-n) \cos\left(\frac{n\pi}{2}\right) S\omega^n \quad (5-6)$$

where $\Gamma(\cdot)$ is the gamma function. For $n < 0.5$ we have $G' > G''$, while for $n > 0.5$ we have $G' < G''$. Figure 5-8 shows the variation of n and S with the molecular weight of polycaprolactone precursors (Izuka et al. 1992). As the molecular weight M_n crosses the entanglement threshold (see Section 3.1), which is around $M_n \approx 6600$, the exponent n drops from near unity to much lower values. Evidently, entanglements among the precursor polymer molecules make the critical gel more elastic, giving it a lower value of n . The exponent n is also affected by the stoichiometric ratio of cross-linker to precursor. Defining r as the molar ratio of cross-linker reactive end groups to precursor reactive end groups, $r = 1$ corresponds to a “balanced” stoichiometry, in which, at complete reaction, there is no excess of either precursor or cross-linker molecules. Figure 5-9b shows that n decreases as the stoichiometric ratio increases towards unity. Thus, the critical gel is more “fluid like,” or dissipative, when there is an excess of precursor end groups (low r).

With increasing r , Fig. 5-9a shows that the decrease in n is accompanied by an increase in the parameter S in Eq. (5-5). At least for some of these critical gels, S can be estimated from the low-frequency modulus G_0 of the fully cured gel and the viscosity η_{sol} of the unreacted sol, or prepolymer, as (Scanlan and Winter 1991)

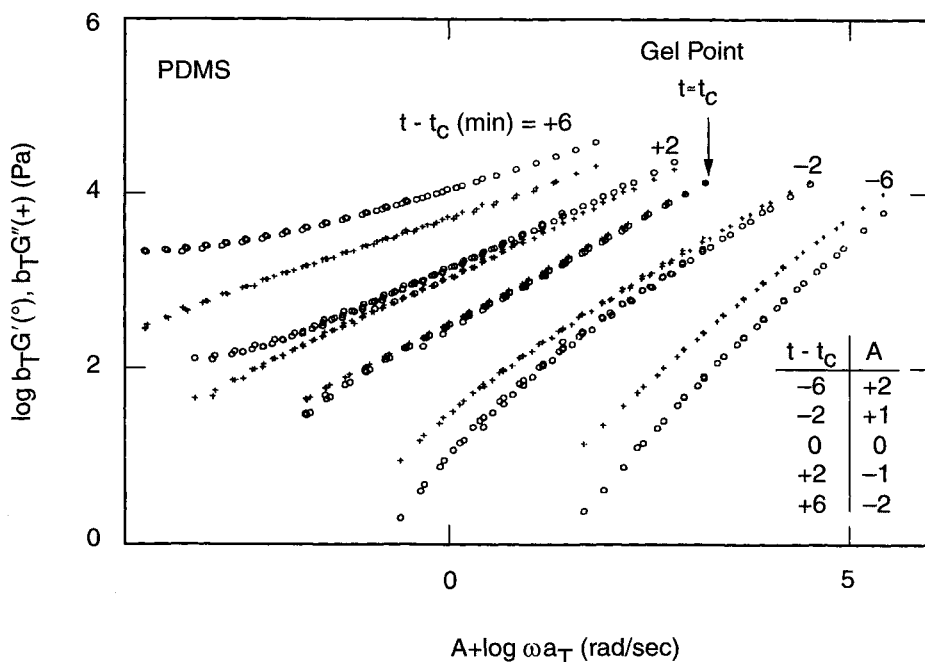


Figure 5.7 Frequency dependences of the storage (○) and loss (+) moduli for poly(dimethylsiloxane) (PDMS) samples whose reactions were quenched at the times indicated (see Fig. 5-6). The data are time-temperature-shifted to the reference temperature T_{ref} of 34°C, and they are shifted additionally by an amount A on the logarithmic axis to keep the curves from overlapping. The vertical shift factors b_T are given by $\rho(T_{ref})T_{ref}/(\rho(T)T)$, where ρ is the density. (From Winter and Chambon 1986, with permission from the Journal of Rheology.)

$$S \approx G_0 \left(\frac{\eta_{sol}}{G_0} \right)^n \quad (5-7)$$

The power laws for viscoelastic spectra near the gel point presumably arise from the fractal scaling properties of gel clusters. Adolf and Martin (1990) have attempted to derive a value for the scaling exponent n from the universal scaling properties of percolation fractal aggregates near the gel point. Using Rouse theory for the dependence of the relaxation time on cluster molecular weight, they obtain $n = D/(2 + D_f) = 2/3$, where $D_f = 2.5$ is the fractal dimensionality of the clusters (see Table 5-1), and $D = 3$ is the dimensionality of space. The theoretical value of $n = 2/3$ agrees with only a small subset of the data published by Winter et al. One system for which $n \approx 2/3$ is observed is a partially cross-linked epoxy system studied by Adolf and Martin (1990) (see Fig. 5-10). For this system, data for samples at various degrees of cure, from the gel point to nearly full cure, can be superposed using *time-cure superposition*, a remarkable law by which the data are shifted horizontally and vertically using the power-law scaling $\tau \propto |p - p_c|^{-3.9}$ and $G_{char} \propto |p - p_c|^{2.8}$ (see Fig. 5-10). These exponents, -3.9 and 2.8 , are close to the values, -4 and $8/3 = 2.67$, derived

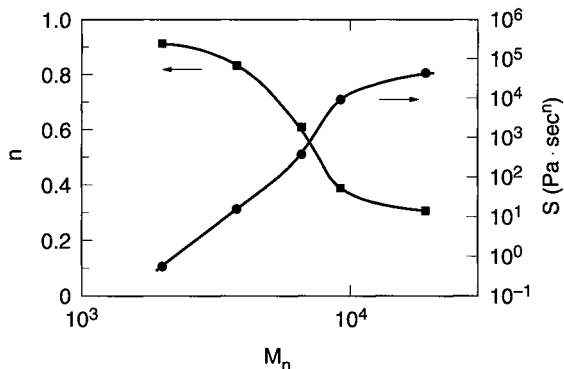


Figure 5.8 Relaxation exponent n and relaxation strength S as functions of the number-average molecular weight of precursor polycaprolactone molecules. (Reprinted with permission from Izuka et al., *Macromolecules* 25:2422. Copyright 1992 American Chemical Society.)

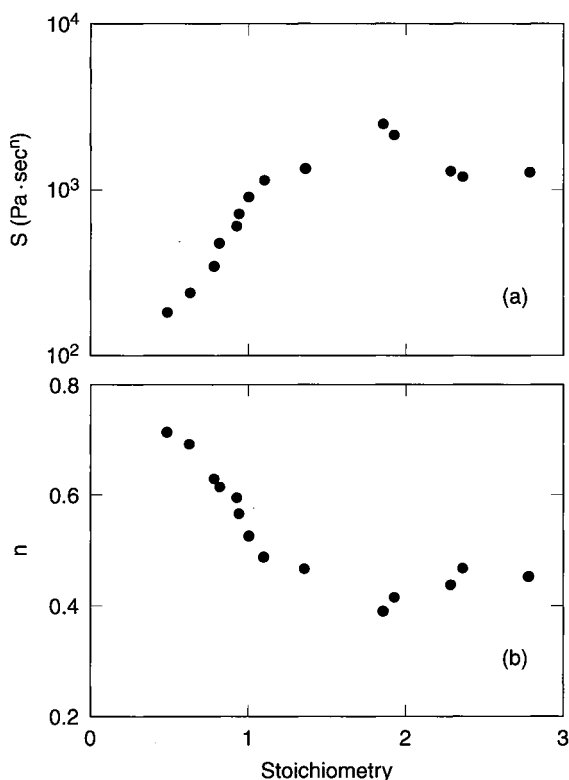


Figure 5.9 (a) Relaxation strength S and (b) relaxation exponent n as functions of stoichiometric ratio r (moles of cross-linker ends/moles of prepolymer ends) for poly(dimethylsiloxane) with prepolymer number-averaged degree of polymerization equal to 142. (Reprinted with permission from Scanlan and Winter, *Macromolecules* 24:47. Copyright 1991 American Chemical Society.)

from “Rouse” theory for gel clusters (Martin and Adolf 1991). Also, the power law for the frequency dependence at the gel point, $G' \propto G'' \propto \omega^{0.72}$, is close to that predicted by the Rouse theory for fractal clusters, $n = 2/3$. An analogous time-cure superposition works for extents of cure less than the gel point, except that then the low-frequency data show terminal (i.e., fluid-like) behavior. The viscosity diverges near the gel point as $\eta_0 \propto |p_c - p|^{1.1}$, where the exponent 1.1 is close to the predicted value $4/3$.

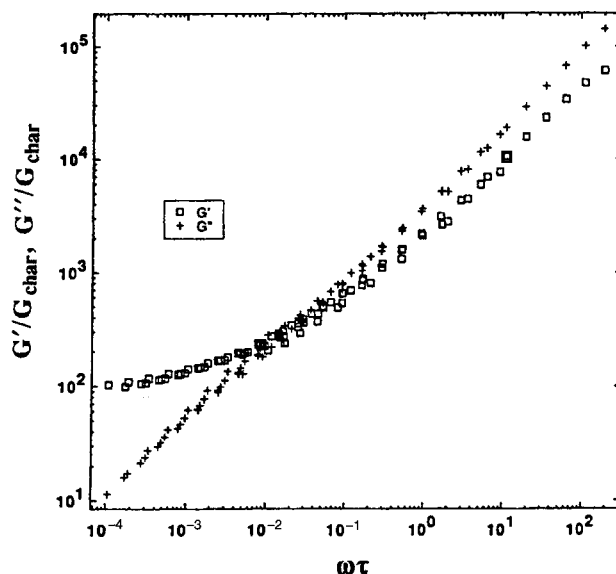


Figure 5.10 Time-cure superposition for a partially cross-linked epoxy obtained by multiplying the frequency ω by $\tau \propto \varepsilon^{-3.9}$ and dividing the moduli G' and G'' by $G_{\text{char}} \propto \varepsilon^{2.8}$, where $\varepsilon \equiv p - p_c$. In the power-law frequency regime, $G' \propto G'' \propto \omega^{0.72}$. (From Martin and Adolf 1991, with permission from the Annual Review of Physical Chemistry, Volume 42, © 1991, by Annual Reviews, Inc.)

However, as remarked earlier, for many gelling systems, particularly those with relatively large precursor molecules, the exponent n can be much less than the theoretical value $n = 2/3$. Winter and Mours (1996) provide a thorough summary of these and other rheological studies of chemical gels.

5.4 RHEOLOGY OF PHYSICAL GELS

We now turn our attention from chemical to physical gels. As mentioned in the Introduction to this chapter, the junctions in physical gels can consist of *locally helical structures*, *microcrystallites*, or *nodular domains*.

Gelation by formation of *helical structures* is still mysterious. Helix formation has been implicated in the gelation of many polymers, including poly(methyl methacrylate) in toluene, bromobenzene, and *o*-xylene (Berghmans et al. 1994; Fazel et al. 1994; Spevacek and Schneider 1974, 1987), isotactic polystyrene in carbon disulfide, *cis*-decalin, *trans*-decalin, and 1-chlorodecane (François et al. 1988; Guenet and McKenna 1988), agarose in water/dimethylsulfoxide (Rochas et al. 1994), and polypeptides in water (Reid et al. 1974; Michon et al. 1993). While a generic “two-step” process for the formation of such gels has been proposed (Berghmans et al. 1994), the precise structure of the intermolecular associations seems to be uncertain. It is clear, however, that tacticity has a strong influence on gel formation; this is consistent with the postulated helix formation. However, even atactic polystyrene can form a gel in many solvents (Tan et al. 1983); thus, even short syndiotactic sequences in atactic polystyrene can induce physical gelation (François et al. 1988). Gelation is often very solvent specific, beyond what can be attributed to generic “solvent quality” (François et al. 1988; Guenet and McKenna 1988). This suggests that solvent–polymer complexes form in at least some cases. For poly(vinyl chloride) in dioctyl phthalate, diethyl

oxalate, esters, and ketones (Alfrey et al. 1949; Mijangos et al. 1993; Lopez et al. 1994), the formation of “sheet-like structures” (presumably analogous to microcrystals) has been postulated as a cause of physical gelation. Molecules with some *rigidity* seem especially prone to physical gelation.

Polymers that form *nodular domains* have specific groups, or “stickers,” attached to them that physically bond with each other, thereby producing physical networks. One class of such associating polymers consists of water-soluble polymers containing hydrophobic groups that huddle together to shield themselves from their aqueous environment. These polymers readily form gel-like networks that greatly enhance the solution viscosity at low concentrations (0.5–5.0 wt%), and thus they are used as “thickeners” in paints, paper coatings, and other such products (Yekta et al. 1995; Karunasena and Glass 1989). Conversely, one can have hydrophobic polymers to which hydrophilic groups are attached; in the melt state the hydrophilic groups associate. For *ionomers*, such as polystyrene sulfonate or sulfonated ethylene-propylene-diene, aggregation occurs via dipole–dipole interactions among ionic groups (Hollday 1983; Eisenberg 1980). Aggregation can also be produced by groups that *hydrogen bond* with each other (Longworth and Morawetz 1958; Stadler and de Lucca Freitas 1986). The enthalpy of formation of a hydrogen bond is on the order of 3–6 kcal/mol, or around 5–10 $k_B T$ per hydrogen bond at room temperature (Pimentel and McClellan 1960). Thus, hydrogen bonds are by no means permanent; but with many such bonds along its backbone, the diffusion of a polymer chain will be drastically slowed down. An example of a hydrogen-bond-forming group is urazole, which, when attached to a polybutadiene chain, leads to the formation of hydrogen-bonded urazole dimers (see Fig. 5-11). Hydrogen-bonding polymers are used as “anti-misting” additives to prevent fuel from ruptured tanks (such as those on damaged airplanes) from atomizing into small, and therefore highly inflammable, droplets (Ballard et al. 1988).

Since attractive interactions between polymer molecules can promote both gelation and phase separation, one might expect phase separation and gelation to occur under similar conditions. Indeed, Fig. 5-12 shows the occurrence of both phase separation and gelation for atactic polystyrene in carbon disulfide. Note that gelation occurs in both the one- and two-phase regions of the phase diagram. If a first-order solid–liquid phase separation occurs by *spinodal decomposition*, the network that forms may be rigid and unable to coarsen, thereby leaving a kinetically trapped gel-like phase (Prasad et al. 1993). That phase separation has occurred may be deduced, however, from sample cloudiness, or from its tendency to undergo *syneresis*, which is the slow exudation of solvent from the gel mass. Even when a network forms without any tendency for bulk phase separation, the formation of infinitely large clusters at the gel point leads to a thermodynamic singularity, which in the model of Tanaka

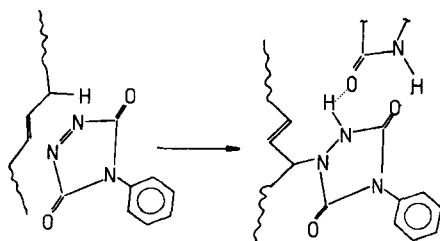


Figure 5.11 A polybutadiene chain reacts with a 4-phenyl-1,2,4-triazoline-3,5-dione group. This group, once attached to the polybutadiene chain, has a hydrogen and an oxygen, both of which can form hydrogen bonds (shown by dashed lines) with the same group on a different chain. (From Stadler and de Lucca Freitas 1986, reprinted with permission from Steinkopff Publishers.)

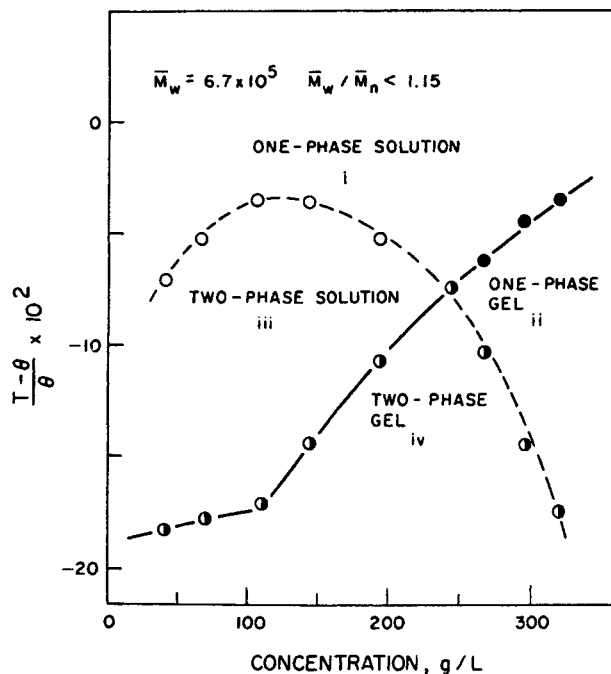


Figure 5.12 Phase diagram of atactic polystyrene in nitropropane. The theta temperature is $\Theta = 200$ K. (Reprinted with permission from Tan et al., *Macromolecules* 16:28. Copyright 1983 American Chemical Society.)

and Stockmayer (1994) is either second or third order, depending on whether the primary chains making up the physical gel are polydisperse or monodisperse. The phase diagrams predicted by the Tanaka–Stockmayer model for physical gelation are qualitatively similar to those observed experimentally (compare Fig. 5-13 with Fig. 5-12).

The subtle relationship between gelation and phase separation is well illustrated by solutions of poly(γ -benzyl-L-glutamate) (PBLG) in solvents such as dimethylformamide (DMF), benzyl alcohol, or toluene. PBLG molecules are stiff, and they form chiral nematic phases when sufficiently concentrated in solution (see Section 2.2.2.1). Figure 5-14a shows the experimental phase diagram for PBLG in DMF, determined by Miller and coworkers using polarimetry and nuclear magnetic resonance (NMR) measurements (Wee and Miller 1971; Miller et al. 1974; see also Tipton and Russo 1996). At high temperatures, there is an isotropic-to-liquid crystal phase transition at polymer volume fractions of around 0.08–0.15, depending on the temperature, with a *narrow* biphasic gap. Both phases at high temperature are fluid, and if the overall composition is in the two-phase “chimney,” they macroscopically separate from each other over time. At lower temperatures, the biphasic gap is huge, and compositions within this wide region form viscous “gels” even when the polymer concentration is as low as 1%! The observed phase diagram is in excellent qualitative agreement with the diagram predicted by Flory (1956) (see Fig. 5-14b). In this theory of Flory, the athermal free energy of rod-like molecules in a solvent is supplemented by a solvent–polymer interaction term, proportional to a parameter χ (see Sections 2.3.1 and 13.2.1). Agreement between theory and experiment is obtained by setting $\chi = -3.51 + 1035/T$, which has a form typical for polymers (see Sections 2.3.1 and

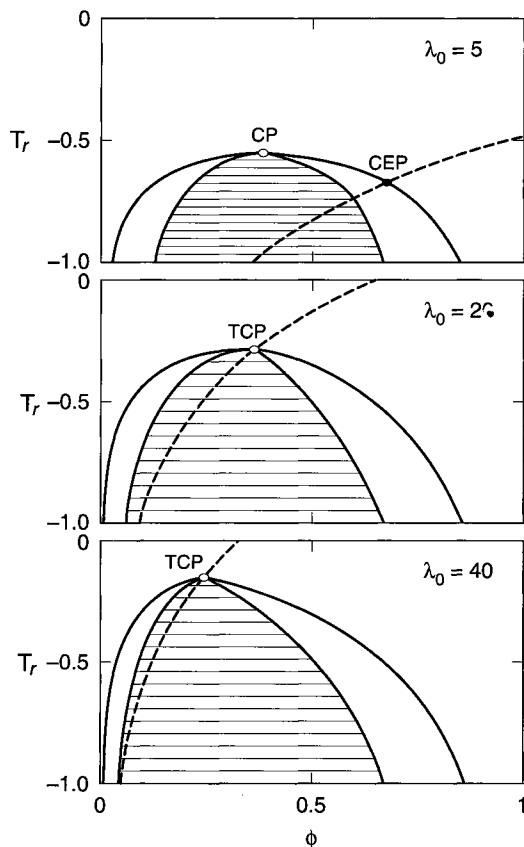


Figure 5.13 Predicted phase diagrams for physical gels made from low-molecular-weight molecules with junctions of unrestricted functionality; ϕ is the total volume fraction of polymer, and T_r is here the reduced distance from the theta temperature, $T_r \equiv 1 - \Theta/T$. The parameter λ_0 controls the equilibrium constant among aggregates of various sizes. The outer solid lines are binodals, the inner solid lines are spinodals, and the dashed lines are gelation transitions. CP is a critical solution point, CEP is a critical end point, and TCP is a tricritical point. (Reprinted with permission from Tanaka and Stockmayer, *Macromolecules* 27:3943. Copyright 1994 American Chemical Society.)

13.2.1). The agreement between theory and experiment supports the conclusion drawn from NMR measurements that the lower region is indeed a two-phase zone, despite the fact that it does not macroscopically phase separate. The implication is that the highly concentrated ordered phase that forms at low temperature is too rigid to separate macroscopically from the solvent, thereby forming a rigid network that pervades the solvent. The resulting material has the rheological properties of a gel (Shukla and Muthukumar 1988). Analogous “gels” form when “waxy crude oil” is cooled, leading to crystallization of the long paraffinic components, which then form a rigid network percolating through the oil, imparting to it a yield stress (Wardhaugh and Boger 1991). Phase-separated “gels” might also occur in flocculated suspensions of rigid spherical particles, to be described in Chapter 7.

In addition to the interesting connections they have to phase-separated systems, physical gels are also similar in some sense to *glasses* (de Gennes 1979; Shukla and Muthukumar 1988). Glasses are disordered solids formed by the progressive freezing of some of the liquid degrees of freedom as the temperature is lowered, resulting in a liquid structure that is too slow to relax on human time scales (see Chapter 4). Physical gelation involves a quenching of mobility due to the formation of a network of bonds that relaxes slowly, if at all. One might suppose that physical gelation can be distinguished from glass formation

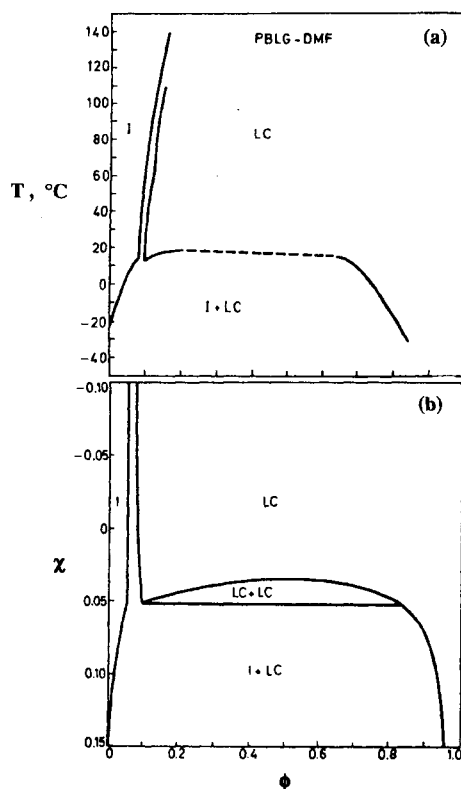


Figure 5.14 (a) Temperature–volume fraction phase diagram for PBLG ($M_w = 310,000$) in DMF, where I denotes an isotropic phase, LC denotes a chiral nematic liquid-crystalline phase, and I + LC is a “gel” that is presumed to be two coexisting phases that are unable to separate macroscopically. (b) The χ -volume fraction phase diagram predicted by the Flory lattice theory for rigid rods of axial ratio (length/diameter) = 150. (From Miller et al. 1974, with permission.)

by the existence in the former of a network; however, so-called strong glasses are also believed to be network formers (see Section 4.2). Thus, conceptually, there is no clear-cut distinction between glasses and gels. It might be helpful to regard gelation and vitrification (or glass formation) as two ends of a continuum. At one extreme, the formation of a network of irreversible chemical bonds can be called *strong gelation* (de Gennes 1979), while the gradual, reversible slowing down of molecular motion due to changes in molecular packing or “free volume” can be called “fragile vitrification,” in accord with Angell’s classification (see Section 4.2). The intermediate case, in which a network of physical bonds forms whose strength is perhaps 5–30 times $k_B T$, could be called either a “weak gel” or a “strong glass.” By convention, a “weak gel” is distinguished from a “strong glass” by the presence in the former of a network of polymer molecules in a solvent, and in the latter of a network of small molecules or ions. Consequently, a glass is typically a hard substance with a higher modulus than a gel.

The rheology of associating polymers can be very complex: They may be solids that fracture under flow, or, conversely, they may be highly fluid at rest and form gels only under flow! The type of behavior depends strongly on the deployment of the stickers along the chain, as well as on molecular weight, concentration, and the method of solution preparation (Pedley et al. 1989). Reproducibility is often a major problem with such materials; for example, samples can “age,” or change slowly over time, especially when ionic groups are

present which might absorb moisture from the atmosphere (Witten 1988). In addition, the presence of associating groups gives the chains an effective attraction for each other that can lead to phase separation, even from a solvent that would be considered “good” in the absence of associations (Witten 1988).

5.4.1 Telechelic Polymers

However, the behavior of one class of associating polymers, the *telechelic polymers*, seems to be reasonably well understood, thanks to recent experimental and theoretical work. Telechelic polymers are linear chains containing associating “sticker” groups only on the chain ends (Jerome et al. 1985). Under steady shear flow, solutions of telechelic polymers typically show a viscosity increase with increasing shear rate (shear thickening), followed by a viscosity decrease (shear thinning) at higher rates.

Examples of telechelic polymers include hydrophobically modified ethoxylated urethanes (HEURs) with hydrophobic end caps consisting of aliphatic alcohols, alkylphenols (Emmons and Stevens 1978; Lundberg et al. 1991), or fluorocarbons (Amis et al. 1996). Figure 5-15 shows a typical structure. The alkane-containing end groups clump together to form nodular “micelles” containing several end groups in aqueous solutions; this substantially enhances the solution viscosity. Further viscosity enhancement, even at a low concentration of HEUR, is achieved by addition of a surfactant. Paints formulated using these components have been found to spatter less when rolled onto surfaces (Lundberg et al. 1991). For a review of the literature on surfactant interactions with associative thickeners, see Winnik and Yekta (1997) and Winnik and Regismond (1996).

The micelles in telechelic polymers differ from micelles formed by typical small-molecule surfactants in that the water-loving “head” groups of telechelic chains are long polymer chains, while in small molecules the head groups are small ionic or hydrophilic nonionic groups. In addition, the telechelic chains have two hydrophobic “tail” groups, one on each end of the hydrophilic chain. In Section 12.3.1, it will be shown that the number of hydrophobic units N_{agg} contained in a micelle is related to the volume v of each hydrophobe and the area a of the micelle surface required to accommodate each hydrophobe within the micelle. The area a is controlled by the bulkiness of the hydrophilic part of the molecule. The formula for N for a spherical micelle is given by [see Eq. (12-9)] $N_{\text{agg}} = 36\pi v^2/a^3$. For an alkane hydrophobe, $v \approx 27n_c \text{ \AA}^3$, where n_c is the number of carbon atoms in the alkane chain [see Eq. (12-1)]. Thus, for $n_c = 16$, we find the relationship $N_{\text{agg}} \approx 20/a^3$, where a is in nm^2 . Because the “head” groups of the telechelic

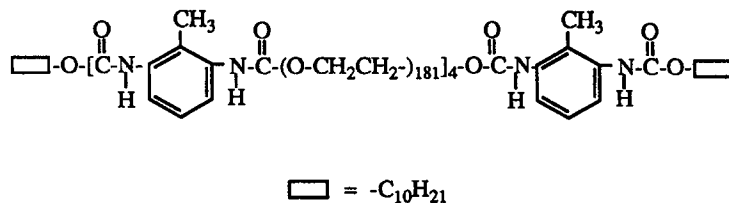


Figure 5.15 Structure of a HEUR polymer. (From Lundberg et al. 1991, with permission from the Journal of Rheology.)

“surfactants” are long, we expect each chain to occupy a large patch of the micelle surface, compared to that occupied by a typical small-molecule surfactant. As a consequence, the aggregation number of telechelic “micelles” should be significantly smaller than that of a small-molecule micelle with a comparably sized hydrophobe. Using fluorescence decay studies, Yekta et al. (1995) have deduced a micelle aggregation number of $N_{\text{agg}} \approx 18\text{--}28$ hydrophobes per micelle, while modeling of rheological data suggests a smaller value, $N_{\text{agg}} \approx 7$ (Annable et al. 1993). These aggregation numbers are much smaller (by a factor of 5–10) than ordinary surfactant micelles with tails of comparable length (see Section 12.3 and Fig. 12-6). Telechelic polymers are also analogous to the *triblock copolymers* discussed in Chapter 13. The difference is in the shortness of the aliphatic “tail” group compared to the block size of typical triblocks. A telechelic polymer is therefore a cross between a surfactant and a block copolymer; it contains two surfactant-sized hydrophobic groups attached to a polymer-sized hydrophilic one.

Because the telechelic polymer has two “tails” or stickers, separated by a long hydrophilic chain, the micelles formed by telechelics are expected to contain “loops” and “bridges,” as depicted in Fig. 5-16. Loops are expected to predominate at concentrations

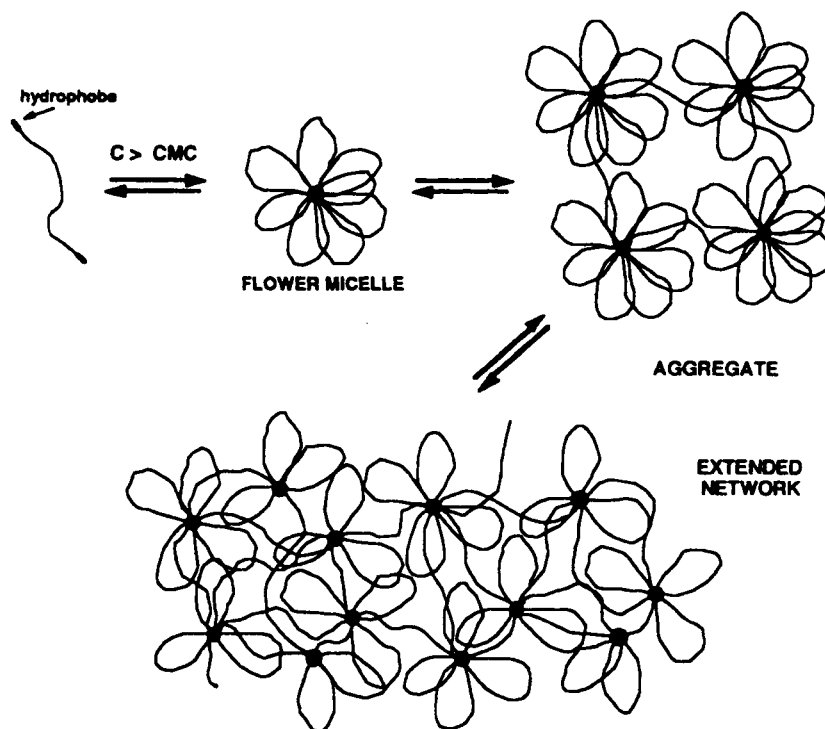


Figure 5.16 Model for associations of telechelic polymers as a function of increasing concentration. For strong associations, isolated “flower” micelles form just above the critical micelle concentration (CMC), which is often around 2 to 10 ppm (Winnick and Yekta 1997). At higher concentrations, the flowers are expected to be connected by “bridges.” (From Winnick and Yekta 1997, with permission from Current Chemistry Ltd.) © 1997 Current Opinion in Colloid + Interface Science.

too low for the hydrophilic chains to bridge between adjacent micelles. These isolated, loop-dominated micelles are called “flowers.” Semenov et al. (1995) have predicted that there is a concentration range where a phase dense in flower micelles separates from a phase lean in them. At very high concentrations (>20 wt%), x-ray scattering and other evidence points to the formation of an ordered cubic array of bridged micelles (Abrahmsen-Alami et al. 1996). As discussed in Chapter 12, similar ordered micellar phases occur in aqueous solutions of ordinary surfactants.

The various types of association that a single telechelic molecule can experience are depicted in Fig. 5-17a. At high enough concentration, one expects networks to form (see Fig. 5-17b). If the molecular weight of the telechelic polymer is low enough, or its concentration in solution is high enough, that the chains do not entangle, then relaxation of a network junction occurs rapidly whenever a sticker group manages to release itself

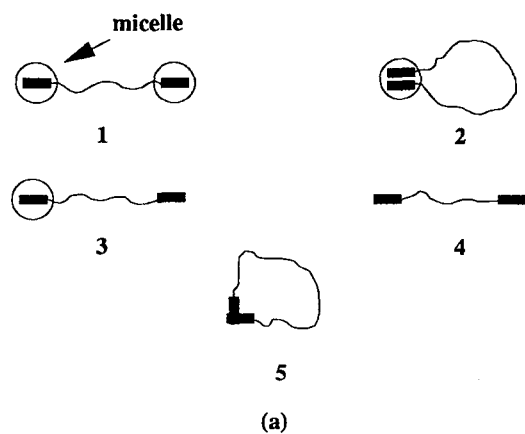
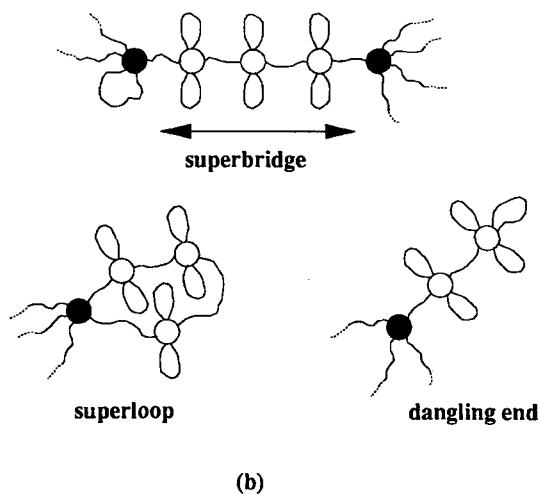


Figure 5.17 (a) Illustration of types of chain association in telechelic polymers. (b) Chain architectures that can form in solution; micelles that have a network functionality greater than two are shown in black. (From Annable et al. 1993, with permission from the Journal of Rheology.)



from one of the micelles. The rheological properties of a such a network are therefore especially simple, as has been shown by Jenkins et al. (1991) and Annable et al. (1993). In particular, for the telechelic polymers studied by Annable et al., the relaxation of the network structure is described by a single-relaxation-time “Maxwell model” (see Fig. 5-18). Such perfect single-relaxation-time behavior is rare. Other known cases of such behavior are for solutions of wormy micelles (discussed in Section 12.3.4), some inorganic glasses (Section 4.8.1), and some dense emulsions (Section 9.3.4). The relaxation time τ of the network is the time constant τ_{diss} for dissociation of a sticker from a micelle, which can be related to the activation barrier energy $\Delta\mu$ for dissociation by

$$\tau_{\text{diss}} = \Omega_0^{-1} e^{\Delta\mu/k_B T} \quad (5-8)$$

where $\Delta\mu$ is the free energy of micellization per sticker, and Ω_0 is a fundamental vibrational frequency, $\Omega_0^{-1} \sim 10^{-10}$ sec (Tanaka and Edwards 1992b). (This free energy difference is roughly equal to the chemical potential difference $\mu_N^0 - \mu_1^0$ for micellization discussed in Section 12.3.1.) For an alkane chain, $\Delta\mu$ increases by roughly $1.5k_B T$ per CH_2 unit. Roughly consistent with this, Annable et al. (1993) found that the relaxation time τ and the zero-shear viscosity η_0 of a typical telechelic HEUR solution increase exponentially with the number of CH_2 units in the sticker, with an increment of around $0.9k_B T$ in $\Delta\mu$ per methylene unit for stickers containing 12–22 CH_2 units.

When $\Delta\mu/k_B T \gg 1$, there will be few free stickers. According to the classical theory for gels, the modulus of a telechelic gel should be simply given by Eq. (5-2), $G_0 = \nu k_B T$,

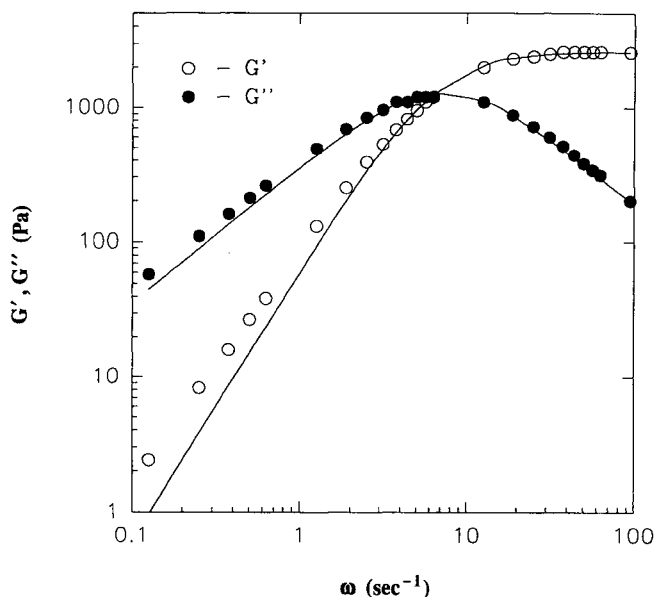


Figure 5.18 Storage and loss moduli for a 7% w/v HEUR associative thickener ($M_w = 33,100$; $M_w/M_n = 1.47$) end-capped with hexadecanol at 25°C . The lines are a fit to a one-mode Maxwell model. (From Annable et al. 1993, with permission from the Journal of Rheology.)

where ν is the number of elastically active chains per unit volume. The zero-shear viscosity is then just $\eta_0 = G_0\tau$. If all chains are elastically “active,” the modulus will be proportional to polymer concentration ν . However, a chain is “active” and contributes to the modulus only if each of its stickers is in a different micelle, as depicted in structure 1 in Fig. 5-17(a). Structure 2 and 5 in Fig. 5-17(a) depict loops which are inactive. If the solution is dilute enough that the chains are, on average, separated from each other by a distance roughly as great or greater than the chain’s radius of gyration, most chains will have to stretch in order to link separate micelles; and thus the probability of loops will be high, so that micelles are mostly unbridged flowers (see Fig. 5-16). Since the radius of gyration is proportional to the square root of the chain’s length, this implies that the probability that a chain is active increases towards unity as the product $c\sqrt{M}$ increases, where c is the concentration of polymer and M is its molecular weight. Figure 5-19a shows that the ratio $G_0/\nu k_B T$ does indeed increase with c , as expected by this argument. The relaxation time also increases with c , as shown in Fig. 5-19b. Annable et al. (1993) argued that τ decreases at low c because the loop formation produces “superbridges” in which $n = 2$ or more chains string

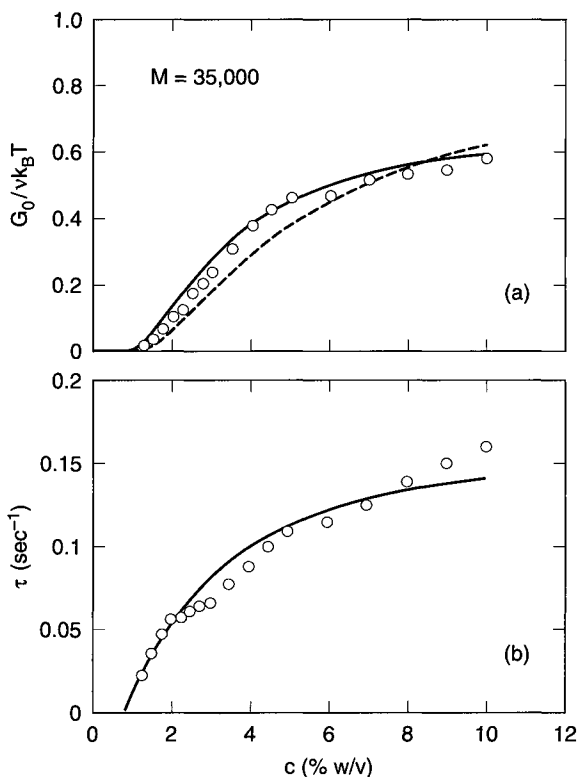


Figure 5.19 (a) The reduced modulus $G_0/\nu k_B T$, and (b) the relaxation time τ , as functions of concentration of the polymer described in the caption to Fig. 5-18. The solid and dashed lines are theoretical predictions assuming, respectively, 70% and 100% for the end-cap efficiencies. (From Annable et al. 1993, with permission from the Journal of Rheology.)

together like paper dolls (see Fig. 5-17b). Since a superbridge is broken when a sticker on any one of the n chains composing it is released from its micelle, the relaxation time is faster by a factor of n than that of a simple bridge. The lines in Fig. 5-19 are predictions of a simple model developed by Annable et al. (1993), which gives good agreement with the measurements. Annable et al. (1993) also confirmed the prediction that τ is a function of the combined variable $c\sqrt{M}$.

A plot of viscosity versus shear rate for a model HUER polymer is shown in Fig. 5-20, and compared to the dynamic viscosity versus frequency. Note that the Cox–Merz rule (see Section 1.3.1.5) fails in that at the frequency ($\omega \approx 1 \text{ sec}^{-1}$) where the dynamic viscosity begins to decrease, the steady shear viscosity begins to *increase* with increasing shear rate, followed by shear thinning at a somewhat higher shear rate. Shear thickening, followed by shear thinning, is often observed in associating polymers (Witten 1988; Marrucci et al. 1993; Hu et al. 1995a; Ketz 1993). The shear thinning can readily be attributed to shear-induced breakup of the gel structure. For stickers whose association energy is significantly greater than $k_B T$, one would expect the gel network to break under shear only when the chains are nearly fully extended. The onset of shear thinning then should occur at a shear rate $\dot{\gamma}_c$ of around $N_K^{1/2}/\tau$, where N_K is the number of “Kuhn steps” in the telechelic polymer, and the relaxation time τ can be estimated by the inverse of the frequency at which the dynamic viscosity begins to shear thin (see Fig. 5-20). This seems to agree with experimental observations (Marrucci et al. 1993).

Figure 5-21 is a plot of the shear viscosity of a HEUR solution, along with superposed illustrations of the structural changes that are believed to occur in the shear-thickening and shear-thinning regions. As explained by Marrucci et al. (1993), weak shear thickening, similar to that shown in Figs. 5-20 and 5-21, can be accounted for by the non-Hookean elastic behavior of network strands that are stretched to more than half their full extension (see Section 3.6.2.2.1). Shear thickening would be expected at shear rates just below those at which shear thinning occurs. Since highly stretched strands pull out of their micelles, only a weak shear-thickening effect can be accounted for by non-Hookean elasticity (Marrucci et al. 1993). Fluorescence studies show that the degree of association of the sticker groups

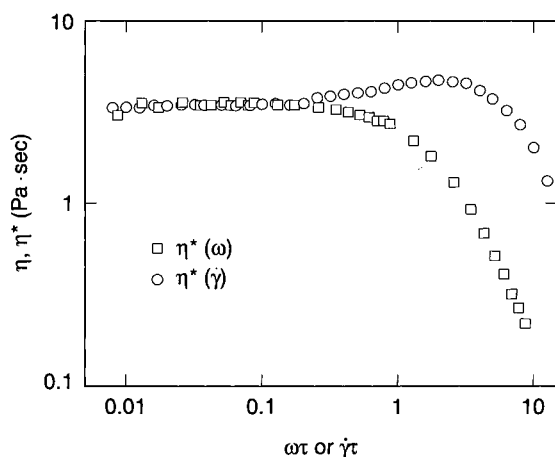


Figure 5.20 Steady-state viscosity $\eta(\dot{\gamma})$ and dynamic complex viscosity $\eta^*(\omega)$ as functions of reduced shear rate ($\dot{\gamma}\tau$) or frequency ($\omega\tau$), for a 1.5% w/v solution of the associative thickener described in the caption to Fig. 5-18. (From Annable et al. 1993, with permission from the Journal of Rheology.)

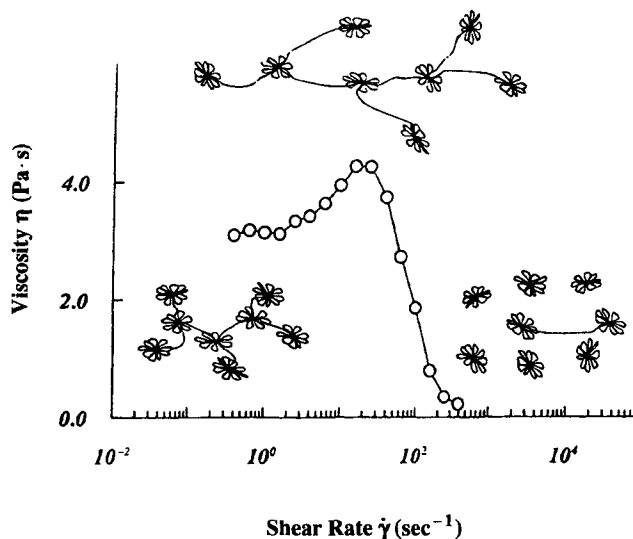


Figure 5.21 Viscosity versus shear rate for 1.0 wt% HEUR ($M_n = 51,000$ $M_w/M_n = 1.7$) telechelic polymers with hexadecanol end caps at 22°C. The illustrations show the structural transitions that are thought to occur as the shear rate is increased. First, the bridging chains are stretched, producing shear thickening. Then, many bridging chains are pulled out at one end from the micelles to which they were attached, and shear thinning occurs. (Reprinted with permission from Yekta et al., *Macromolecules* 28:956. Copyright 1995 American Chemical Society.)

does not change over the shear-rate range depicted in Fig. 5-21 (Yekta et al. 1995). This would seem to imply that the decrease in bridging that occurs in the shear-thinning region is accompanied by an increase in loop formation, so that free ends are avoided. Thus, at high shear rates, “flowers” may predominate.

Some associating polymers show very strong shear thickening, with the viscosity increasing by more than an order of magnitude over a narrow range of shear rates. Massive shear thickening of this kind seems to be common in polymers with many stickers distributed along each chain. We discuss the behavior of such polymers in the next section. We end this section by noting that Tanaka and Edwards (1992a, 1992b) and Marrucci et al. (1993) have developed promising temporary-network kinetic models for telechelic polymers, by applying ideas originally formulated by Green and Tobolsky (1946) and Yamamoto (1956, 1958) (see Section 3.4.2).

5.4.2 Entangled “Sticky” Chains

Telechelic polymers have stickers only on their ends, and they are often of small enough molecular weight to be unentangled. There are, of course, many other ways of deploying stickers on a polymer. There can be several, or many, stickers, arranged either regularly or randomly along the chain. The stickers can be attached directly to the polymer backbone, or they can be offset by a nonsticky “spacer” (Winnik and Yekta 1997). Clever balancing

of various constituents can lead to unusual solution properties with important technological applications. An example is “hydrophobic alkali-swellaible emulsion” (HASE) polymers that contain carboxylic and acrylate ester groups in a composition balanced so that the polymer collapses into an insoluble ball at low pH, but at pH > 6 it expands and dissolves (Jenkins et al. 1996; Winnik and Yekta 1997).

A simpler case to consider theoretically is that of many associating sites more or less regularly spaced along the contour of a chain that is long enough and concentrated enough to be entangled with other chains. An example is the melt of polybutadiene with randomly attached urazole groups studied by Stadler and de Lucca Freitas (1986, 1989). Each urazole group is apparently capable of forming two hydrogen bonds with another such group. Figure 5-22 shows G' as a function of reduced frequency for polybutadiene with various mole percentages of attached urazole groups. The added urazole groups dramatically slow down the relaxation, and change the shape of the curve, such that transition to true terminal behavior (for which $G' \propto \omega^2$) becomes more gradual. This change in the shape of G' versus ω at low frequency is reminiscent of that produced by molecular-weight polydispersity.

The frequency-dependent loss modulus for such samples often has two peaks. One of the peaks corresponds to the longest relaxation time of the molecule; this peak shifts to lower frequency (longer relaxation time) as the number of urazole groups per chain increases. The second peak occurs at a frequency of around $2 \times 10^4 \text{ sec}^{-1}$ at 0°C and is independent of the number of urazole groups. This frequency appears to correspond to the inverse lifetime of an association between two urazole groups. The presence of a time constant that is much longer than the association lifetime makes this many-sticker system differ markedly from the telechelic chains discussed in Section 5.4.1. For unentangled telechelics, the relaxation

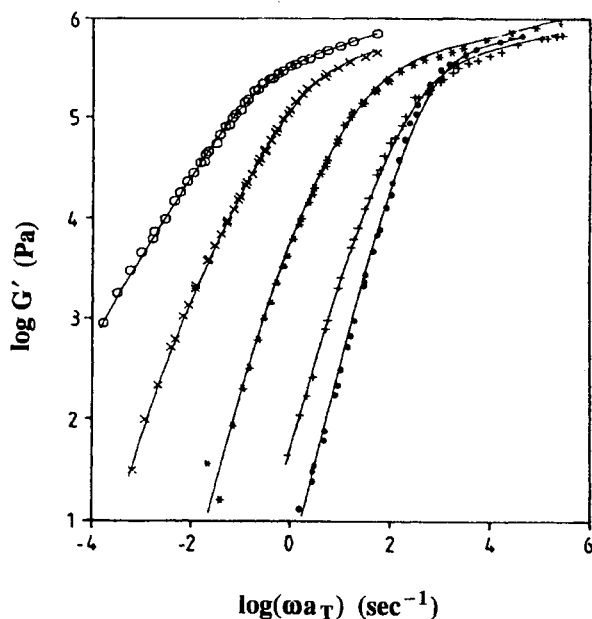


Figure 5.22 Master curves of the storage modulus at a reduced temperature of 0°C for polybutadiene ($M_n = 26,000$) which has been modified by attachment of 4-phenyl-1,2,4-triazoline-3,5-dione groups, as illustrated in Fig. 5-11. The degree of modification is $x = 0$ (●), 0.5 (+), 2 (*), 5 (×), and 7.5 (○), where $x = 7.5$ corresponds to 36 functional groups per chain. (Reprinted with permission from de Lucca Freitas and Stadler, *Macromolecules* 20:2478. Copyright 1987 American Chemical Society.)

time constant of the gel is either equal to or less than the time a sticker spends in an association.

This difference presumably exists because, for multisticker chains, the dissociation of one sticker from another does not permit relaxation of the entire chain, since the chain is anchored in place by many other stickers, and because it is confined by entanglements with other chains to a “tube-like” region (see Section 3.7). The other stickers and entanglements prevent the chain from diffusing very far before any newly released sticker is captured by a new association (see Fig. 5-23). Thus, one might expect that the chain can only relax its conformations during those exponentially rare moments when all stickers are released. However, Ballard et al. (1988) pointed out that a chain with many stickers can move like a *centipede*: at any one time only a few of the centipede’s legs are moving freely, but since the animal is somewhat flexible and each leg eventually gets a turn to move, the whole animal can slowly creep forward. Likewise, even if only a small fraction of its stickers are free to move at any one instant, the polymer molecule can alter its shape and center-of-mass position slightly to accommodate the movement of a few stickers. Over time the whole chain slowly moves back and forth in its tube, like a drunken centipede in a maze, and slowly relaxes its configuration, even though at no time are all the stickers released.

Leibler et al. (1991) have developed a model for this process, which they call “sticky reptation.” For long chains with many stickers, the self-diffusion coefficient of a sticky reptating chain turns out to be

$$D_{\text{self}} \approx \frac{a^2}{2\tau_{\text{diss}}S^2} \left(1 - \frac{9}{p} + \frac{12}{p^2} \right) \quad (5-9)$$

where a is the reptation “tube diameter” (see Section 3.7), S is the number of stickers per chain, p is the average fraction of stickers that are associated at a given time, and τ_{diss} is the lifetime of the association. Apart from the factor involving p , Eq. (5-9) is analogous to the corresponding formula for ordinary reptation, $D_{\text{self}} = (a^2/\tau_e)(N_e/N)^2$, with S in Eq. (5-9) playing the role of the number of entanglements per chain, N/N_e , and τ_{diss} in Eq. (5-9) playing the role of the equilibration time of a chain segment between entanglement points, τ_e (see Section 3.7.4.2). Here, as elsewhere, N is the number of monomers per macromolecule and N_e is the number of monomers in an entanglement spacing.

For a chain moving by reptation or by “sticky reptation,” one expects the reptation time, which scales roughly as the 3.5 power of N , to be related to the diffusion coefficient (which scales as N^{-2}), by

$$\tau \approx \left(\frac{N}{N_e} \right)^{1.5} \frac{a^2}{D_{\text{self}}} = \left(\frac{N}{N_e} \right)^{1.5} \frac{2S^2\tau_{\text{diss}}}{1 - 9/p + 12/p^2} \quad (5-10)$$

The predictions of Eq. (5-10) are in good agreement with measured τ values for urazole-modified polybutadienes (Leibler et al. 1991).

The plateau modulus is given by the usual formula for entangled polymers, $G_0^N \approx \nu k_B T$, where ν is the number of entanglement strands per unit volume of melt; that is, $\nu = N\nu_m/N_e$, where ν_m is the number of molecules per unit volume, $\nu_m = \rho N_A/M$, N_A is Avogadro’s number, ρ is the melt density, and M is the chain’s molecular weight. The zero-shear viscosity is estimated to be simply $\eta_0 \approx G_0^N \tau$, as usual.

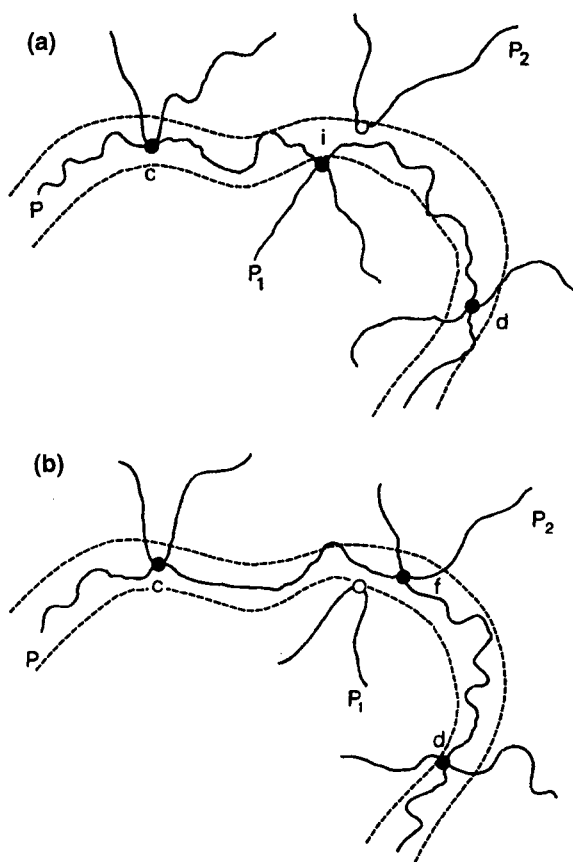


Figure 5.23 “Sticky reptation”: In (a) the chain P is cross-linked to chain P₁ at point *i*, but in (b), it has released this cross-link and attached itself to chain P₂ at point *f*. (Reprinted with permission from Leibler et al., *Macromolecules* 24:4701. Copyright 1991 American Chemical Society.)

Shear thickening in polymers with multiple stickers is thought to be caused by a shear-induced change in the balance between intramolecular and intermolecular associations (Witten and Cohen 1985). According to this idea, at low shear rates, many of the associations are *intramolecular* and therefore contribute little or nothing to the viscosity. Shearing flow stretches the molecules, and thus it makes intermolecular associations more probable. The result is an increase in viscosity. The increase in viscosity causes the chain to stretch even more, and this promotes even more interchain associations. The result can be a runaway increase in the viscosity, or *shear-induced gel formation*.

While this mechanism for shear thickening is plausible, it has not yet been confirmed by direct probes of the association behavior of the chains. Pedley et al. (1989) found that shear thickening in such systems is not accompanied by any measurable change in average extension of the chains. This could imply that only a small fraction of chains participate in the shear-induced thickening phenomenon, while the rest remain balled up in self-aggregated clusters (Marrucci et al. 1993). Witten (1988) has argued that chains with associations strong enough to produce dramatic shear-thickening effects are likely to be prone to phase separation. This may explain the poor reproducibility and sensitivity to sample preparation frequently experienced with these solutions.

Severe shear thickening is most likely to occur for multisticker, entangled chains. For such chains, relaxation after a sticker is released is slower than reassociation, so that chains reassociate while still in a stretched state, and very high viscosities can then build up. In short unentangled telechelic polymers, on the other hand, chain relaxation is expected to be fast enough that chains are unstretched when they reassociate, and the shear thickening is then modest.

5.5 SUMMARY

Chemical gels, and perhaps physical gels also, show power-law frequency-dependences of the linear viscoelastic moduli G' and G'' at the transition from sol to gel, and thus the spectrum can be characterized completely by a power law exponent n and a relaxation strength S . The constants n and S vary systematically with molecular weight of the prepolymer and with the ratio of prepolymer to cross-linker.

The rheological properties of physical gels, which have associating groups along their backbones or on their ends, are, on the whole, not yet well-understood, in part because of their sensitivity to preparation and poor reproducibility. However, much progress has recently been made toward understanding the rheology of telechelic polymers, which have associating groups or “stickers” only on their ends. Telechelic polymers seem to be describable by a temporary network model in which the relaxation is dominated by the rate of release of stickers from the micelles to which they are associated. Molecules with many stickers along their backbone have rheological properties that depend on the number of such sticker groups as well as the sticker release rate. It might be possible to model the rheology of long molecules with many stickers by the “sticky reptation” model of Leibler et al. Under steady shear, telechelics and other associating polymers usually show shear thickening, followed at higher shear rate by shear thinning. The shear thinning is probably caused by stress-induced breakdown of the network. A weak shear-thickening phenomenon can be explained by non-Gaussian chain statistics, but massive shear-thickening or shear-induced gelation seems to imply that intermolecular associations can be enhanced by shearing flow.

REFERENCES

- Abrahmsen-Alami S, Alami E, François F (1996). *J Colloid Interface Sci* 179:20.
 Adolf D, Martin JE (1990). *Macromolecules* 23:3700.
 Alfrey T, Wiederhorn N, Stein RS, Tobolsky AV (1949). *Ind Eng Chem* 41:701.
 Amis EJ, Hu N, Seery TAP, Hogen-Esch TE, Yassini M, Hwang F (1996). In *Hydrophilic Polymers, Performance with Environmental Acceptability*, Glass JE (ed), American Chemical Society, Washington, DC.
 Annable T, Buscall R, Ettelaie R, Whittlestone D (1993). *J Rheol* 37:695.
 Arbabi S, Sahimi M (1988). *Phys Rev B* 38:7173.
 Ballard MJ, Buscall R, Waite FA (1988). *Polymer* 29:1287.
 Berghmans M, Thijs S, Cornette M, Berghmans H, De Schryver FC, Moldenaers P, Mewis J (1994). *Macromolecules* 27:7669.
 Brinker CJ, Scherer GW (1990). *Sol-Gel Science: The Physics and Chemistry of Sol-Gel Processing*, Academic Press, New York.
 Broadbent SR, Hammersley JM (1957). *Proc Camb Philos Soc* 53:629.

- Chambon F, Petrovic ZS, MacKnight, Winter HH (1986). *Macromolecules* 19:2146.
- Chiou B-S, English RJ, Khan SA (1996). *Macromolecules* 29:5368.
- de Gennes PG (1976). *J Phys (Paris) Lett* 37L:61.
- de Gennes PG (1979). *Scaling Concepts in Polymer Physics*, Cornell University Press, Ithaca, NY.
- de Lucca Freitas L, Stadler R (1987). *Macromolecules* 20:2478.
- Eisenberg A (ed) (1980). *Ions in Polymers*, Advances in Chemistry Series 187, American Chemical Society, Washington, DC.
- Eliassaf J, Silberberg A, Katchalsky A (1955). *Nature* 176:1119.
- Emmons WD, Stevens TS (1978). US Patent 4,079,028.
- Erman B, Flory PJ (1983). *Macromolecules* 16:1600.
- Fazel N, Brulet A, Guenet J-M (1994). *Macromolecules* 27:3836.
- Ferry JD (1980). *Viscoelastic Properties of Polymers*, 3rd ed, Wiley, New York.
- Fisher ME, Essam JW (1961). *J Math Phys* 2:609.
- Flory PJ (1941). *J Am Chem Soc* 63:3083.
- Flory PJ (1942). *J Phys Chem* 46:132.
- Flory PJ (1953). *Principles of Polymer Chemistry*, Cornell University Press, Ithaca, NY.
- Flory PJ (1956). *Proc R Soc (Lond)* A234:73.
- François J, Gan J, Sarazin D, Guenet J-M (1988). *Polymer* 29:898.
- Green MS, Tobolsky AV (1946). *J Chem Phys* 14:80.
- Guenet J-M (1992). *Thermoreversible Gelation of Polymers and Biopolymers*, Academic Press, London.
- Guenet J-M, McKenna GB (1988). *Macromolecules* 21:1752.
- Hess W, Vilgis TA, Winter HH (1988). *Macromolecules* 21:2536.
- Hollday L (ed) (1983). *Developments in Ionic Polymers*, Applied Science, London.
- Horkay F, McKenna GB (1996). In *Physical Properties of Polymers Handbook*, Mark JE (ed), AIP Press, New York.
- Hu Y, Wang SQ, Jamieson AM (1995a). *Macromolecules* 28:1847.
- Hu Z, Zhang X, Li Y (1995b). *Science* 269:525.
- Izuka A, Winter HH, Hashimoto T (1992). *Macromolecules* 25:2422.
- James HM, Guth E (1953). *J Chem Phys* 21:1039.
- Jenkins RC, Silebi CA, El-Asser MS (1991). *ACS Symp Ser* 462:222-233.
- Jenkins RC, DeLong LM, Bassett DR (1996). In *Hydrophilic Polymers* Glass JE (ed), ACS Advances in Chemistry Series 248, American Chemical Society, Washington, DC.
- Jerome R, Broze G, Teyssie P (1985). In *Microdomains in Polymer Solutions*, Dubin P (ed), Plenum Press, New York.
- Karunasena A, Glass JE (1989). *Prog Org Coatings* 17:301.
- Ketz RJ Jr (1993). PhD Thesis, Princeton University.
- Kirkpatrick S (1973). *Rev Mod Phys* 45:574.
- Larson RG, Davis HT (1982). *J Phys C Solid State Phys* 15:2327.
- Leibler L, Rubinstein M, Colby RH (1991). *Macromolecules* 24:4701.
- Lodge A (1961). *Polymer* 2:195.
- Longworth R, Morawetz H (1958). *J Polym Sci* 29:307.
- Lopez D, Dahmani M, Mijangos C, Brûlet A, Guenet J-M (1994). *Macromolecules* 27:7415.
- Lundberg DJ, Glass JE, Eley RR (1991). *J Rheol* 35:1255.
- Marrucci G, Bhargava S, Cooper SL (1993). *Macromolecules* 26:6483.
- Martin JE, Adolf D (1991). *Annu Rev Phys Chem* 42:311.
- Menchen S, Winnik MA (1994). US Patent 5,290,418.
- Menchen S, Johnson B, Winnik MA, Xu B (1996). *Electrophoresis* 17:1451.
- Michon C, Couvelier G, Launay B (1993). *Rheol Acta* 32:94.

- Mijangos C, López D, Muñoz ME, Santamaría A (1993). *Macromolecules* 26:5693.
- Miller WG, Wu CC, Wee EL, Santee GL, Rai JH, Goebel KG (1974). *Pure Appl Chem* 38:37.
- Mooney M (1940). *J Appl Phys* 11:582.
- Osada Y, Ross-Murphy SB (1993). *Sci Am*, May: 82.
- Pedley AM, Higgins JS, Peiffer DG, Rennie AR, Staples E (1989). *Polymer Comm* 30:162.
- Peterlin A, Turner DT (1965). *J Polym Sci Polym Lett* 3:517.
- Pimentel GC, McClellan AC (1960). *The Hydrogen Bond*, WH Freeman, San Francisco.
- Prasad A, Marand H, Mandelkern L (1993). *J Polym Sci Polym Phys Ed* 32:1819.
- Reid DS, Bryce TA, Clark AH, Rees DA (1974). *Faraday Discuss* 57:230.
- Richtering HW, Gagnon KD, Lenz RW, Fuller RC, Winter HH (1992). *Macromolecules* 25:2429.
- Rivlin RS (1948). *Philos Trans R Soc A* 241:379.
- Rochas C, Brulet A, Guenet J-M (1994). *Macromolecules* 27:3830.
- Scanlan JC, Winter HH (1991). *Macromolecules* 24:47.
- Semenov AN, Joanny J-F, Khokhlov AR (1995). *Macromolecules* 28:1066.
- Shante VKS, Kirkpatrick S (1971). *Adv Phys* 20:325.
- Shukla P, Muthukumar M (1988). *Polym Eng Sci* 28:1304.
- Spevacek J, Schneider B (1974). *Makromolekul Chem* 175:2939.
- Spevacek J, Schneider B (1987). *Colloid Interface Sci* 27:81.
- Stadler R, de Lucca Freitas L (1986). *Colloid Polym Sci* 264:773.
- Stadler R, de Lucca Freitas L (1989). *Makromol Chem Macro Symp* 26:451.
- Stauffer D (1976). *J Chem Soc Faraday Trans II* 72:1354.
- Stinchcombe RB (1974). *J Phys C Solid State Phys* 7:179.
- Stockmayer WH (1943). *J Chem Phys* 11:45.
- Straley JP (1977). *J Phys C Solid State Phys* 10:3009.
- Straley JP (1982). *J Phys C Solid State Phys* 15:2333.
- Tan H-M, Moet A, Hiltner A, Baer E (1983). *Macromolecules* 16:28.
- Tanaka T (1981). *Sci Amer* 244:124.
- Tanaka F, Edwards SF (1992a). *Macromolecules* 25:7003.
- Tanaka F, Edwards SF (1992b). *J Non-Newt Fluid Mech* 43:247,273,289.
- Tanaka F, Stockmayer WH (1994). *Macromolecules* 27:3943.
- Tipton DL, Russo PS (1996). *Macromolecules* 29:7402.
- Treloar LRG (1975). *The Physics of Rubber Elasticity*, 3rd ed, Clarendon Press, Oxford.
- Vallés EM, Macosko CW (1979). *Macromolecules* 12:521.
- Venkataraman SK, Coyne L, Chambon F, Gottlieb M, Winter HH, (1989). *Polymer* 30:2222.
- Wall FT (1943). *J Chem Phys* 11:527.
- Wardhaugh LT, Boger DV (1991). *J Rheol* 35:1121.
- Wee EL, Miller WG (1971). *J Phys Chem* 75:1446.
- Winnik MA, Regismond STA (1996). *Colloid Surf A* 118:1.
- Winnik MA, Yekta A (1997). *Curr Opin Colloid Interface Sci* 2:424.
- Winter HH (1989). In *Encyclopedia of Polymer Science and Engineering*, Supplement Volume, Second ed, Wiley, New York.
- Winter HH, Chambon (1986). *J Rheol* 30:367.
- Winter HH, Morganelli P, Chambon F (1988). *Macromolecules* 21:532.
- Winter HH, Mours M (1997). *Adv Polym Sci* 134:165.
- Witten TA Jr, Cohen MH (1985). *Macromolecules* 18:1915.
- Witten TA (1988). *J Phys (France)* 49:1055.
- Yamamoto M (1956). *J Phys Soc Jp* 11:413.
- Yamamoto M (1958). *J Phys Soc Jp* 13:1200.
- Yekta A, Xu B, Duhamel J, Adiwidjaja H, Winnik MA (1995). *Macromolecules* 28:956.
- Zosel A (1991). *J Adhesion* 34:201.